

Figure 4. Packing model for alkyl chains in $M(\text{O}_3\text{PC}_n\text{H}_{2n+1})\cdot\text{H}_2\text{O}$. The angle between the P-C bond and the c axis (83°) is taken from the $\text{Mn}(\text{O}_3\text{PC}_6\text{H}_5)\cdot\text{H}_2\text{O}$ structure. The tilt angle τ is the angle between the c axis and the alkyl chain axis.

are added to the chain. From the angle between the P-C bond and the ac plane in $\text{Mn}(\text{O}_3\text{PC}_6\text{H}_5)\cdot\text{H}_2\text{O}$ (82.7°) and an average C-C-C bond angle²² of $111-112^\circ$, we anticipate an "ideal" tilt angle τ , the angle between the chain axis and the ac plane, of approximately 49° . From the C-C single bond distance (1.53 \AA) we calculate an average increase in b of 1.91 \AA per carbon atom added to the chain. Experimentally, we observe in the Mg series $\Delta b/\Delta n = 1.78 \text{ \AA}$ for C_1-C_3 and 1.99 \AA for C_4-C_{12} , implying tilt angles of 45 and 52° , respectively. That the tilt angle is smaller for C_1-C_3 than for C_4-C_{12} follows from a packing model shown

(22) (a) Wyckoff, R. W. G. *Crystal Structures*; Wiley-Interscience: New York, 1966; Vol. 5, pp 589-612. (b) Kitaigorodskii, A. I. *Molecular Crystals and Molecules*; Academic: New York, 1973; pp 48-62.

in Figure 4. The n th carbon atom in a given chain makes closest contact with the $n+3$ carbon in a neighboring chain (related by a c axis translation). For C_1-C_3 there is no $n+3$ carbon, and the smaller tilt angle allows more efficient packing of the alkyl groups.

For $\text{C}_{\geq 4}$, the avoided $n, n+3$ contacts cause the tilt angle to increase. Even with the higher tilt angle, unreasonably close ($<3.0 \text{ \AA}$) $\text{C}_n, \text{C}_{n+3}$ contacts are calculated if all carbon atoms are forced to lie in the mirror (bc) planes. There is, however, sufficient room in the structure for the chains to twist out of these planes via rotation about P-C and C-C bonds: the chain width²² perpendicular to the bc plane is ca. 4.0 \AA , but the a axis spacing (the separation distance between chains) is 5.7 \AA . It is reasonable that the chains might twist alternately above and below the mirror planes, while maintaining an approximately all-trans configuration, as shown in Figure 4. Calculations of alkyl chain density²³ for $\text{Mg}(\text{O}_3\text{PR})\cdot\text{H}_2\text{O}$ give an average value of 0.85 g/cm^3 . This is comparable to the densities of crystalline n -alkanes, e.g. $\text{CH}_3(\text{C}-\text{H}_2)_{16}\text{CH}_3$ (0.78 g/cm^3), $\text{CH}_3(\text{CH}_2)_{20}\text{CH}_3$ (0.79 g/cm^3), and $\text{CH}_3(\text{CH}_2)_{34}\text{CH}_3$ (0.96 g/cm^3), and suggests that the chains are packed reasonably efficiently despite the long (5.7 \AA) separation distance between them along the a axis.

Acknowledgment. This work was supported by grants from the Research Corp., the Texas Advanced Technology Research Program, and the Robert A. Welch Foundation.

Supplementary Material Available: For $\text{Mn}(\text{O}_3\text{PC}_6\text{H}_5)\cdot\text{H}_2\text{O}$ refined in space group $Pmn2_1$, listings of anisotropic thermal parameters, hydrogen coordinates, and hydrogen bond angles and distances (Supplementary Tables I-IV) (2 pages); a listing of observed and calculated structure factor amplitudes (Supplementary Table V) (2 pages). Ordering information is given on any current masthead page.

(23) The average chain density of the C_1-C_{12} compounds in the $\text{Mg}(\text{O}_3\text{PR})\cdot\text{H}_2\text{O}$ series is calculated as

$$\rho = [2M_r(\text{C}_{11}\text{H}_{22})]/[6.022 \times 10^{23}ac(b_{\text{C}_{12}} - b_{\text{C}_1})]$$

Contribution from the Instituto de Ciencia de Materiales CSIC, Serrano 115 dpdo, 28006 Madrid, Spain

Proton-Sodium Exchange in Magadiite. Spectroscopic Study (NMR, IR) of the Evolution of Interlayer OH Groups

J. M. Rojo,* E. Ruiz-Hitzky, and J. Sanz

Received December 14, 1987

The formation process of the layered silicic acid H-magadiite, obtained after hydrochloric acid treatment of magadiite, has been studied by IR and (^1H and ^{23}Na) NMR spectroscopies combined with X-ray diffraction, chemical, and thermogravimetric analyses. This study shows that magadiite is a hydrogen silicate of layer structure, in which the negative charge of the layers is compensated by sodium ions or by protons ($\text{Si}-\text{O}^-\text{Na}^+/\text{Si}-\text{OH}$ ratio $\sim 2/3$). The progressive exchange of sodium ions by protons decreases the average H-H distance between OH groups from $\sim 4 \text{ \AA}$ in magadiite to $\sim 2.5 \text{ \AA}$ in H-magadiite. When all the sodium ions have been exchanged, the silicic structure collapses as a consequence of the establishment of hydrogen bonds between adjacent layers. These interactions prevent the interlayer water adsorption in H-magadiite.

Introduction

The mineral magadiite, first described by Eugster¹ as a sodium layered silicate, is available as a powder with an average particle size of $1-2 \text{ \mu m}$ and can be easily synthesized under hydrothermal conditions.^{2,3} By acid treatment, sodium ions are exchanged by protons, yielding the layered silicic acid called H-magadiite in a topotactic process. Although the crystalline structures of both magadiite and H-magadiite are unknown at the present, ^{29}Si NMR spectroscopy has allowed us to identify two types of SiO_4 tet-

rahedra:^{4,5} those within the layers sharing four oxygens with neighboring SiO_4 tetrahedra and those located at the interlamellar surface that share three oxygens with other tetrahedra and bear one OH group. Silanol groups in H-magadiite have been characterized by IR and ^1H NMR spectroscopies, showing two types of OH groups: those that are involved in relatively strong hydrogen bonds between adjacent layers and those more free, probably pointing to holes of the next layers.⁶ The two types of OH groups

(1) Eugster, H. P. *Science (Washington, D.C.)* **1967**, *157*, 1177.

(2) McCulloch, L. *J. Am. Chem. Soc.* **1952**, *74*, 2453.

(3) Lagaly, G.; Beneke, K.; Weiss, A. *Proc. Int. Clay Conf.*, **1972**, *1972*, 663.

(4) Rojo, J. M.; Sanz, J.; Ruiz-Hitzky, E.; Serratos, J. M. *Z. Anorg. Allg. Chem.* **1986**, *540/541*, 227.

(5) Pinnavaia, T. J.; Johnson, I. D.; Lipsicas, M. *J. Solid State Chem.* **1986**, *63*, 118.

(6) Rojo, J. M.; Ruiz-Hitzky, E.; Sanz, J.; Serratos, J. M. *Rev. Chim. Miner.* **1983**, *20*, 807.

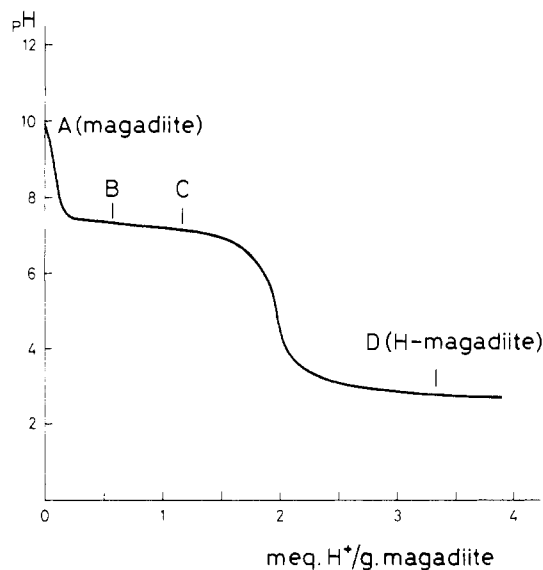


Figure 1. Titration curve of magadiite with a 0.01 N HCl solution. pH is plotted versus amount of acid added to a suspension of 70 mg of magadiite in 10 mL of water.

are located in the interlayer space and are involved in the interlamellar adsorption of organic molecules⁷ and in the intracrystalline grafting reactions of organosilanes.^{8,9}

The aim of this work is to analyze by IR and (²³Na and ¹H) NMR spectroscopies the formation process of the silicic acid H-magadiite. In particular, we have studied the evolution of the different types of OH groups and sodium ions present in the interlayer space of magadiite during the acid treatment of this silicate.

Experimental Section

The magadiite used in this work is a natural sample from Trinity County, CA. The titration curve of magadiite has been obtained by using an automatic buret coupled to a Radiometer Copenhagen RTS 822 pH meter. About 70 mg of silicate was dispersed in 10 mL of water and titrated under continuous stirring at 25 °C with a 0.01 N HCl solution. The sodium content of the samples was determined by extraction of Na⁺ ions with diluted HCl and analysis of the corresponding solutions with an Eppendorf flame spectrophotometer. The SiO₂ content was determined by conventional chemical analysis (gravimetric and atomic absorption methods). Thermogravimetric curves were obtained with a Mettler instrument, at a heating rate of 10 °C/min.

X-ray diffractograms were obtained with a Philips Model PW 1010 instrument equipped with a Cu anode and Ni filter. The scanning rate was 1°/min for 3 < 2θ < 60°. The samples were examined as self-supporting oriented films.

IR spectra were recorded on a Perkin-Elmer Model 580B double-beam spectrophotometer coupled to a PE M-3500 data station. Samples (films of thin wafers of approximately 2 mg/cm²) were examined in a typical vacuum cell with CaF₂ windows in order to prevent the rehydration of the samples during the thermal treatments.

Pulse ¹H NMR spectra were obtained in an SXP 4/100 Bruker instrument using a working frequency of 70 MHz. NMR data were processed on an Aspect 2000 computer equipped with a suitable fast Fourier system that allowed by successive accumulations a signal/noise ratio better than 30. The samples were formed by superimposing individual plaques from oriented aggregated films on the interior of a square-section Pyrex cell designed to conserve the degree of hydration. This procedure allowed the sample orientation to be changed relative to the external magnetic field. High-resolution ²³Na MAS NMR spectra were recorded at 105.8 MHz with a Bruker MSL 400 spectrometer. The spinning frequency of the samples was 4.8 kHz. A diluted aqueous solution of NaCl was used as an external reference. Cross polarization and proton decoupling were not used. A time interval of 2 s between successive accumulations was selected to avoid saturation effects. Accumulations

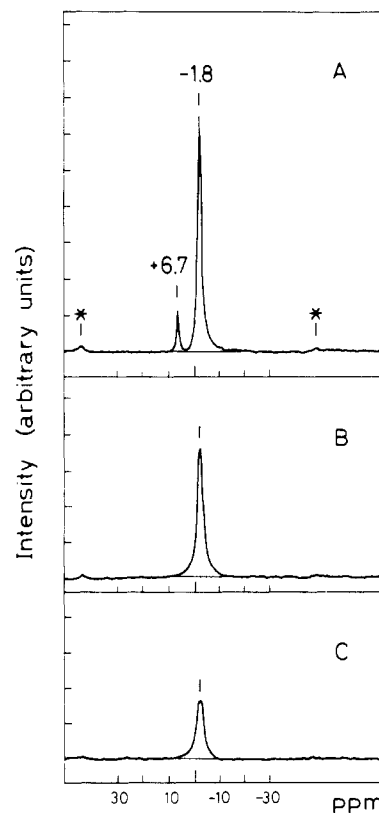


Figure 2. ²³Na NMR spectra of samples A (magadiite), B, and C (asterisks, indicate spinning sidebands).

amounted to 100 fid's. All spectra were recorded at room temperature.

Results

Titration Curve. The titration curve of magadiite with hydrochloric acid (Figure 1) is similar to that described by Lagaly,¹⁰ showing two different steps: one in which the pH dispersion changes from 9.8 to ~7 and other in which it changes from ~7 to 2.5. Samples A and D in Figure 1 are magadiite and H-magadiite, respectively, while B and C correspond to intermediate stages of the titration process. The four samples have been studied by IR and NMR spectroscopies; ²³Na NMR spectroscopy makes it possible to identify different kinds of sodium in magadiite, and ¹H NMR and IR spectroscopies make it possible to follow the formation of new OH groups.

NMR Spectroscopy. (a) ²³Na NMR spectra of samples A, B, and C are represented in Figure 2. The spectrum of sample A shows two signals, of different intensity, at +6.7 and -1.8 ppm. The first signal is not observed in the spectrum of sample B, i.e. when the pH dispersion is ~7. The frequency of the second signal does not appreciably change in the three spectra, but the intensity progressively decreases upon going from sample A to C. This signal disappears from the spectrum in sample D. The sodium content of the silicate, during the acid treatment, was deduced from the total intensity of the spectrum in each sample.

(b) The evolution of ¹H NMR spectra corresponding to the four samples heated at different temperatures is shown in Figure 3. The spectra of samples A, B, and C, recorded at 20 °C when the sample plaques are disposed perpendicular to the magnetic field, present a single signal with a full width at half-maximum (fwhm) of 0.4 G. When these samples are heated at 110 °C, the intensity of the signal centered at the resonance frequency decreases and two doublets with component separations of 6 and 3 G are observed. These doublets are eliminated in the range 110–300 °C, first the 6-G doublet (110–170 °C) and then the 3-G doublet (170–300 °C). The dehydration of these samples is accompanied by a decrease in the basal spacing from 15.5 to 11.4 Å, which is attributed to the elimination of water molecules adsorbed in the

(7) Rojo, J. M.; Ruiz-Hitzky, E. *J. Chim. Phys. Phys.-Chim. Biol.* **1984**, *81*, 625.

(8) Ruiz-Hitzky, E.; Rojo, J. M. *Nature (London)* **1980**, *287*, 28.

(9) Ruiz-Hitzky, E.; Rojo, J. M.; Lagaly, G. *Colloid Polym. Sci.* **1985**, *263*, 1025.

(10) Lagaly, G. *Adv. Colloid Interface Sci.* **1979**, *11*, 105.

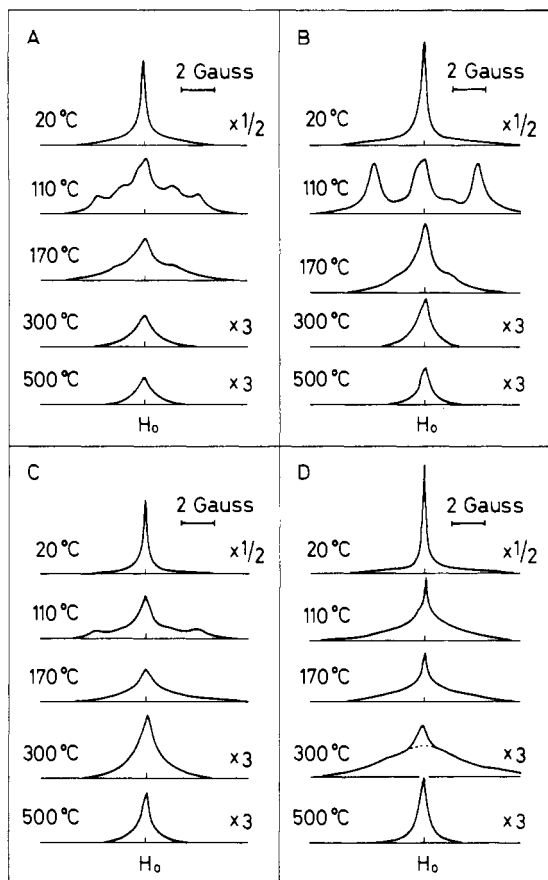


Figure 3. ^1H NMR spectra of samples A (magadiite), B, C, and D (H-magadiite) treated at increasing temperatures.

interlayer space. On the contrary, in sample D, the same thermal treatment does not affect the basal spacing (11.2 Å) and the ^1H NMR spectra show exclusively the elimination of a narrow component centered at the resonance frequency, which corresponds to water adsorbed at the external surface of this compound.

The evolution of the spectra as a function of the sample orientation with respect to the external magnetic field made it possible¹¹ to assign the two doublets to two types of water molecules. The separation of the doublet at 6 G (type I) decreases to 3 G, overlapping with the 3-G doublet (type II), when the magnetic field changes from a perpendicular to a parallel orientation with respect to the sample plaques. The 3-G doublet is not sensitive to the magnetic field orientation.

NMR spectra of the samples heated at 300 °C, i.e. when the adsorbed water has been completely eliminated, show only one signal assigned to OH groups, whose intensity increases from samples A to D. The signal of sample D consists of two components centered at the resonance frequency, one whose fwhm is 0.7 G and other whose intensity is greater, with a fwhm of 5.1 G, which is not present in the spectra of samples A, B, and C. When the four samples are heated between 300 and 500 °C, a decrease in intensity of the ^1H NMR signals is observed due to the partial condensation of OH groups. These signals are eliminated in the range between 500 and 1000 °C.

IR Spectroscopy. Infrared spectra of the samples heated at increasing temperatures are shown in Figure 4. The spectra of samples A, B, and C at 20 °C show different bands in the 4000–2500- cm^{-1} region (stretching vibrations ν_{OH}) and two bands at 1670 and 1630 cm^{-1} (bending vibrations $\delta_{\text{H-O-H}}$) assigned to two types of water in the silicate. The thermal treatment produces the elimination at different temperatures of both bands. However, the continuous and similar decrease of all the bands in the 4000–2500- cm^{-1} region precludes the identification of the stretching bands associated with the two different types of water.

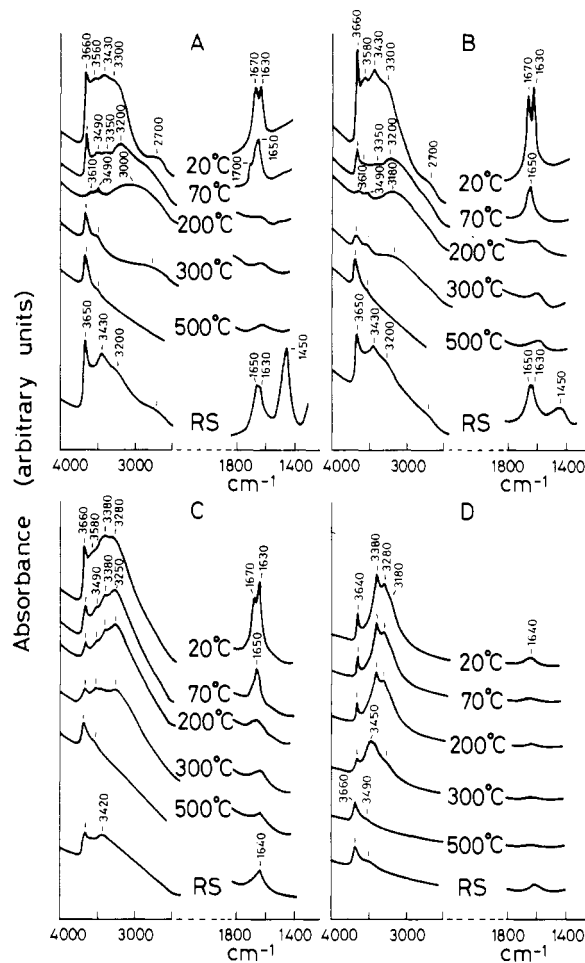


Figure 4. IR spectra of samples A (magadiite), B, C, and D (H-magadiite) treated at increasing temperatures. The spectra labeled as RS are those of the rehydrated samples after heating at 500 °C.

The comparison of the spectra of the four dehydrated samples (200 °C) affords information about the evolution of the OH groups in the interlayer space of magadiite during the acid treatment. Thus, the spectrum of magadiite presents two bands at 3660–3610 and 3490 cm^{-1} and an additional broad band centered at 3000 cm^{-1} ; this band is narrowed and shifted toward higher frequencies (3180 cm^{-1}) by acid treatment (Figure 4B). The spectrum of sample C shows new bands at 3380 and 3280–3250 cm^{-1} , typical of the silicic acid H-magadiite, which become narrower and more intense in the spectrum of sample D.

When samples A, B, and C are heated between 200 and 500 °C, the bands at lower frequencies (3400–3000- cm^{-1} region) are eliminated, and an increase in intensity of the bands at 3660 and 3490 cm^{-1} is observed. In sample D, the same thermal treatment produces the elimination of the low-frequency bands (3380, 3280, and 3180 cm^{-1}); however, the intensity of the higher frequency bands (3660 and 3490 cm^{-1}) is almost unaffected.

On the other hand, the spectrum of sample A, when it is heated at 500 °C and subsequently exposed to the atmosphere, shows two bands at 1630 and 1650 cm^{-1} , which are assigned to water readsorbed in the silicate, and a new band at 1450 cm^{-1} , which is assigned to asymmetric stretching vibrations of carbonate ions.¹² The intensity of this band decreases with the previous acid treatment of the sample, disappearing from the spectrum of sample C.

XRD and TG Analysis. Figure 5 shows the X-ray diffractograms of the four samples. The X-ray diffraction pattern of sample B is similar to that of magadiite (sample A), and in both cases the basal spacing is 15.5 Å. The diffractogram of sample

(11) Rojo, J. M. Ph.D. Thesis, University Complutense Madrid, 1983.

(12) Farmer, V. C. *The Infrared Spectra of Minerals*; Mineralogical Society: London, 1974.

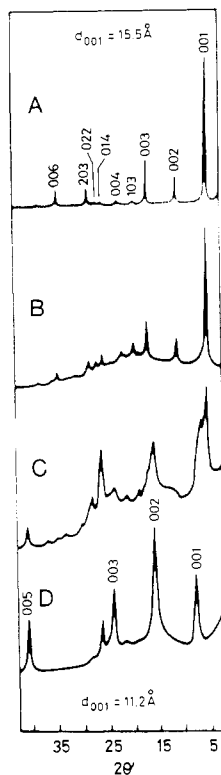


Figure 5. X-ray diffraction patterns obtained on self-supporting oriented films of samples A, B, C, and D. The peaks have been assigned according to Brindley.¹⁸

C shows peaks characteristic of samples A and D; moreover, some disorder in the stacking of individual layers of silicate is detected, as indicated by the peak broadening in the X-ray diffraction pattern. When the silicic acid is formed (sample D), the basal spacing becomes 11.2 Å.

Thermogravimetric curves of the samples are shown in Figure 6. The weight losses in the ranges 20–250 and 250–1000 °C are due to the elimination of water and OH groups, respectively. The amount of water retained by the silicate decreases slowly from samples A to C, being very low in the case of sample D. The quantity of OH groups lost increases upon going from sample A to D. A change of slope between 350 and 550 °C is observed in the curves of samples B, C, and D, indicating that the dehydroxylation process occurs in two steps: the first one corresponding to the condensation of OH groups assigned in the IR spectra to ν_{OH} bands at low frequencies (3400–3000 cm^{-1}) and the second corresponding to OH groups that give stretching bands at higher frequencies (above 3400 cm^{-1}). In the case of sample A, the differentiation between both dehydroxylation steps is not clear.

Discussion

The X-ray diffractogram of magadiite obtained from H-magadiite treated with a diluted solution of sodium hydroxide coincides with that of the starting natural silicate, showing that the moderate acidic or basic treatment of magadiite and H-magadiite, respectively, does not alter the structure of the silicic layers. This fact is confirmed by ^{29}Si NMR spectra⁵ of magadiite and H-magadiite, in which the two signals, assigned to Si surrounded by 4 Si and Si surrounded by 3 Si and 1 Na^+ or 1 OH, have the same intensity ratio.

The titration of magadiite with diluted hydrochloric acid is not a simple process since it occurs in two different steps. The first one, in which the pH dispersion changes from 9.8 to ~ 7 , should be associated with the neutralization of an excess of sodium hydroxide adsorbed in the silicate, and the second step, in which the pH changes from ~ 7 to 2.5, with the exchange of sodium ions by protons in the structure.

This interpretation is supported by IR and NMR spectroscopies. Thus, the signal at 6.7 ppm in the ^{23}Na NMR spectrum of sample A (Figure 2), assigned to Na^+ of sodium hydroxide, disappears

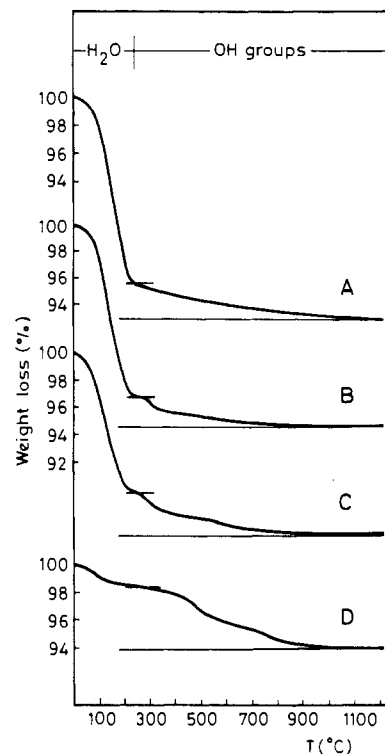


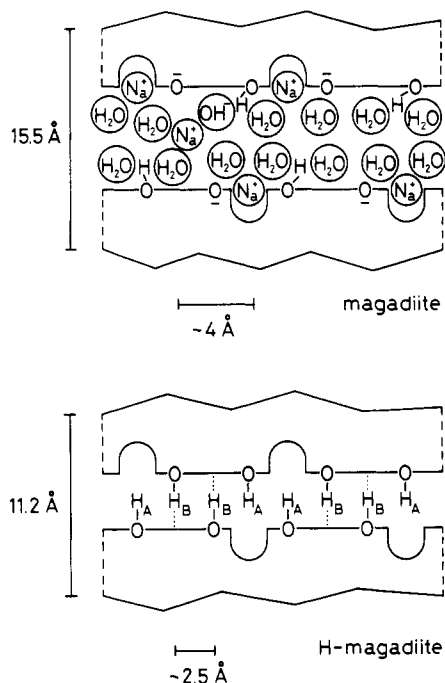
Figure 6. Thermogravimetric curves of samples A (magadiite), B, C, and D (H-magadiite).

from the spectrum in sample B. Besides, the band at 1450 cm^{-1} , observed after rehydration of sample A in the IR spectrum and assigned to asymmetric stretching vibrations of carbonate ions,¹² also evidences the presence of sodium hydroxide species that react with atmospheric CO_2 . This band almost disappears from the spectrum of sample B, i.e. when the pH dispersion is close to 7. The presence of sodium hydroxide in magadiite, even when this sample has been washed several times, and the absence in the X-ray diffractogram of the characteristic reflections of crystalline sodium hydroxide suggest that part of these species should be adsorbed in the interlamellar space of this silicate. On the other hand, the IR spectrum of dehydrated sample A at 200 °C (Figure 4) shows two bands at 3610 and 3490 cm^{-1} , which increase in intensity when the broad band at 3000 cm^{-1} is eliminated during the heating of the sample between 200 and 500 °C. This behavior can be explained by assuming that the band at 3000 cm^{-1} corresponds to silanol groups in interaction with interlayer sodium hydroxide. When this interaction is eliminated by partial dehydroxylation of the sample, the silanol groups are detected at higher frequencies. These results, in agreement with those of NMR spectroscopy (^1H signal), prove the existence of a considerable amount of silanol groups in magadiite, which must be considered as a hydrogen silicate with a $\text{Si-O}^-\text{Na}^+/\text{Si-OH}$ ratio close to 2/3 (Table I). The relative amount of sodium as $\text{Si-O}^-\text{Na}^+$ and NaOH was determined on the basis that H-magadiite (sample D) has 5.2 OH groups per 14 Si.⁴ The quantity of NaOH deduced by chemical analysis is in complete agreement with that determined from the intensity of the signal at 6.7 ppm in the ^{23}Na NMR spectrum of sample A.

A scheme of the interlayer space of magadiite consistent with the above results is represented in Figure 7. In this model, the negative charge of SiO_4 tetrahedra pointing out of the layers is compensated by sodium ions or protons. From a comparison of the basal spacing of the hydrated and dehydrated samples ($\Delta d_1 = 4.1$ Å), it can be concluded that the water molecules are disposed in a bilayer arrangement. The detection in this phase of one type of water with high mobility and another one strongly linked to sodium ions makes unfavorable the idea that cations are positioned in the center of the interlamellar space, used to explain the observed bilayer arrangement. The presence of sodium hydroxide is probably related to the fact that magadiite is formed in strong

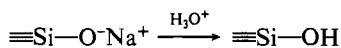
Table I. Chemical Composition of Samples A, B, C, and D and Relative Sodium Content (%) Deduced from ^{23}Na NMR Spectroscopy and Conventional Chemical Analysis

sample	chem formula		^{23}Na NMR	chem anal.
A (magadiite)	$\text{H}_{3.1}\text{Na}_{2.1}\text{Si}_{14}\text{O}_{30.6}$	0.25NaOH	8.4H ₂ O	100
B	$\text{H}_{3.5}\text{Na}_{1.7}\text{Si}_{14}\text{O}_{30.6}$		7.6H ₂ O	69
C	$\text{H}_{4.1}\text{Na}_{1.1}\text{Si}_{14}\text{O}_{30.6}$		5.9H ₂ O	39
D (H-magadiite)	$\text{H}_{5.2}\text{Si}_{14}\text{O}_{30.6}$		0.8H ₂ O	0

**Figure 7.** Schematic representation of the interlayer space of magadiite and H-magadiite.

alkali media,^{1,2} which favors the adsorption of an additional amount of these species. However, the coexistence of weakly acidic silanol groups and sodium hydroxide can only be explained by the difficulty in transforming all the Si-OH in SiO⁻Na⁺ groups.^{13,14} This fact also explains why magadiite is a hydrogen silicate, similar to other layer silicates reported in the literature.^{15,16} However, the model of interlayer space here presented is different from those proposed by other authors: Eugster¹ considers that magadiite is composed of alternating sodium hydroxide and silica sheets, and Lagaly et al.¹⁷ suggest that the negative charge of the layers is compensated by sodium and do not consider the existence of silanol groups in this silicate. In sample B, the sodium hydroxide is mostly neutralized and only a few new Si-OH groups are formed.

In the first plateau of the titration curve, where the pH dispersion is almost constant (pH ~7), new silanol groups are produced as a consequence of the exchange of sodium ions by protons:



Thus, the intensity of the signal at -1.8 ppm, assigned to sodium of Si-O⁻Na⁺ groups, progressively decreases in the ^{23}Na NMR spectra of samples B and C (Figure 2), while the intensity of the ^1H NMR signal, due to OH groups, increases upon going from samples B to C and C to D (Figure 3). In addition, the IR spectrum of dehydrated sample C shows new stretching ν_{OH} bands at 3380, 3280-3250, and 3180 cm⁻¹, characteristic of silanol groups

of the silicic acid H-magadiite (Figure 4). In sample C, where sodium ions have been partially exchanged by protons, the X-ray diffractogram shows typical peaks for magadiite and H-magadiite, indicating the coexistence of the two phases. When all the sodium ions have been exchanged by protons, the pH dispersion reaches the value of the hydrochloric acid solution used in the titration process.

The progressive exchange of sodium ions by protons produces a continuous elimination of the two doublets detected by ^1H NMR spectroscopy and associated with interlayer water coordinated to sodium ions. This fact shows that these ions are mainly responsible for the presence of water in the interlamellar space. In the case of sample D, in which all the sodium ions have been exchanged by protons, the basal spacing decreases to 11.2 Å and water is exclusively adsorbed at the external surface of H-magadiite.

During the acid treatment, the quantity of OH groups located in the interlayer surface increases, and when it becomes high enough (sample D), the structure spontaneously collapses, which indicates that the OH groups have more tendency to establish hydrogen bonds with oxygens of the next layers than with water molecules. The decrease of the basal spacing from 15.5 to 11.2 Å produces (Figure 7) a clear differentiation of the silanol groups in two types: one more free (OH_A), probably pointing to holes defined by tetrahedral rings of the next layers, and the other one (OH_B) involved in relatively strong hydrogen bonds between adjacent layers, which are responsible for the interlamellar cohesion. In agreement with this interpretation, the IR spectrum of sample D shows bands at 3660-3640 and 3490 cm⁻¹, which have been assigned⁶ to stretching ν_{OH} vibrations of OH_A groups, and bands at 3380, 3280, and 3180 cm⁻¹, due to OH_B groups.

Contrary to the case of H-magadiite obtained from natural silicate, the layer silicic acid prepared from a synthetic magadiite retains an appreciable amount of water. The basal spacing ($d_1 = 13.2$ Å) corresponds to the presence of a monolayer of water molecules in the interlamellar space of this compound. The observed difference proves that the interlamellar cohesion, derived from the establishment of hydrogen bonds between adjacent layers, is weaker in the synthetic silicic acid. This is confirmed by IR spectroscopy;⁶ the stretching ν_{OH} band assigned to hydrogen-bonded OH_B groups of this sample is detected at higher frequency (3440 cm⁻¹) than in the case of silicic acid obtained from the natural silicate. These facts show that the two silicic acids are different, probably due to a poorer crystallinity of the synthetic material. In this way, data from the ^{29}Si NMR spectra^{4,5} suggest that the condensation degree of SiO₄ tetrahedra within the layers is different in both silicic acids.

From the analysis of the second moment of the ^1H NMR signal, the average H-H distances between neighboring protons can be deduced.⁶ This method demonstrates a decrease of the distances between OH groups from ~4 Å in sample A to ~2.5 Å in sample D. Taking into account that the surface density of OH groups in sample D is ~3.5 OH/100 Å², as deduced from the OH content and the interlayer surface area,¹¹ we calculate that the average H-H distance between nearest neighboring protons should be 4.6 Å for a homogeneous distribution of OH groups. As the value deduced from the ^1H NMR signal is ~2.5 Å, it is evident that OH groups must be preferentially distributed in certain directions of the interlamellar surface. Moreover, not having each SiO₄ tetrahedron with more than one OH group⁴ requires that H-H distances smaller than 3 Å must be necessarily between OH groups belonging to superimposing tetrahedra of adjacent layers.

Finally, the quantity and distribution of interlayer OH groups have a significant influence on the adsorption properties of the thermally treated samples. Thus, when sample D is heated be-

- (13) Heston, W. M.; Iler, R. K.; Sears, G. W. *J. Phys. Chem.* **1960**, *64*, 147.
 (14) Allen, L. H.; Matijevic, E. *J. Colloid Interface Sci.* **1969**, *31*, 287.
 (15) Le Bihan, M. T.; Kalt, A.; Wey, R. *Bull. Soc. Fr. Mineral. Cristallogr.* **1971**, *94*, 15.
 (16) Johan, Z.; Maglione, G. F. *Bull. Soc. Fr. Mineral. Cristallogr.* **1972**, *95*, 371.
 (17) Lagaly, G.; Beneke, K.; Weiss, A. *Am. Mineral.* **1975**, *60*, 642.
 (18) Brindley, G. W. *Am. Mineral.* **1969**, *54*, 1583.

tween 200 and 500 °C, OH_β groups are mostly eliminated, giving Si-O-Si bridges between layers, which prevent interlayer rehydration and sorption of organic molecules.⁶ In sample C, in which the amount of OH groups is lower than in sample D, the capability of rehydration is higher. However, the same thermal treatment of samples A and B does not preclude the subsequent interlayer rehydration and carbonation (basal spacing 14.2 Å), as deduced from infrared and X-ray data. Therefore, it is clear that the interlayer sodium hinders the formation of Si-O-Si bridges between silanol groups of adjacent layers, during the thermal treatment of the samples.

Conclusions

Magadiite is a sodium hydrated hydrogen silicate of lamellar structure that has an excess of sodium hydroxide adsorbed to it. The layers are built up by condensation of two silica tetrahedral sheets,^{4,5} and the negative charge of the SiO₄ tetrahedra pointing out of the layer is compensated by sodium ions or by protons, which give silanol groups. The relative proportion of these Si-O⁻Na⁺ and Si-OH groups is approximately 2/3.

The acid treatment of magadiite produces first the neutralization of adsorbed sodium hydroxide and then the exchange of sodium by protons, yielding new Si-OH groups. This treatment increases the interlayer surface density of silanol groups, and the average H-H distances between these groups decrease from ~4 Å in magadiite to ~2.5 Å in H-magadiite. When the silicic acid H-magadiite is obtained, the structure collapses, producing a clear differentiation of the OH groups in two types: those involved in hydrogen bonding between adjacent layers and those that do not interact with the tetrahedral sheet of contiguous layers.

Finally, it is worthwhile to note that silanol groups with both characteristics, short H-H distances and participation in relatively strong hydrogen bonds, have never been observed in amorphous silica and are the consequence of an ordered arrangement of the adjacent layers in the silicic acid H-magadiite.

Acknowledgment. This work was partially supported by a grant from the CAICYT of Spain. We thank Prof. J. M. Serratosa for helpful discussions.

Registry No. Na, 7440-23-5; HCl, 7647-01-0; magadiite, 12285-88-0.

Contribution from the Department of Chemistry, Northwestern University, Evanston, Illinois 60208

New Soluble Monomeric Polyselenide Anions, [MQ(Se₄)₂]²⁻ (M = Mo, W; Q = O, S, Se)

Robert W. M. Wardle, Charles H. Mahler, Chung-Nin Chau, and James A. Ibers*

Received December 23, 1987

Reaction of MO₄²⁻ (M = Mo, W) with [(CH₃)₂(CH₃(CH₂)₇)Si]₂Se provides a new synthetic route to the tetraselenometalates MSe₄²⁻. Reaction of MSe₄²⁻ with Se₈, SeS₂, or Se₄(NC₅H₁₀)₂ affords the MQ(Se₄)₂²⁻ ion with Q = Se, S, or O, respectively. ⁷⁷Se NMR studies of this system confirm the general assignment trends of terminal Se (>1200 ppm), "metal bound" Se (1200-600 ppm), and ring Se (<600 ppm). The M = Mo series resonates at lower field than does the M = W series. These trends are in agreement with those seen in ¹⁷O and previous ⁷⁷Se NMR studies. The compound [NEt₄]₂[MoO(Se₄)₂] crystallizes in the monoclinic space group P₂₁/c with a = 9.287 (2) Å, b = 17.132 (4) Å, c = 18.353 (4) Å, β = 97.38 (1)°, and Z = 4. The MoO(Se₄)₂²⁻ ion shows square-pyramidal coordination of the Mo^{IV} center by the apical O atom and the two bidentate Se₄²⁻ units. [PPh₄]₂[WS(Se₄)₂] crystallizes in the monoclinic space group P₂₁/a with a = 18.366 (7) Å, b = 12.873 (6) Å, c = 20.666 (8) Å, β = 100.74 (1)°, and Z = 4. WS(Se₄)₂²⁻ is structurally analogous to MoO(Se₄)₂²⁻. All of the MSe₄ (M = Mo, W) rings exhibit conformations similar to that of cyclopentane.

Introduction

The relatively rare soluble transition-metal selenide anions (M_xSe_y^{z-}) that are currently known in some instances have no direct counterparts among the more common sulfide anions. Those that are analogous to known sulfides include MoSe₄²⁻¹ (vs MoS₄²⁻²), WSe₄²⁻³ (vs WS₄²⁻²), Fe₂Se₁₂²⁻⁴ (vs Fe₂S₁₂²⁻⁴), W₃Se₂²⁻ and W₃OSe₈²⁻⁵ (vs W₃S₉²⁻ and W₃OS₈²⁻⁶), and the unsymmetrical isomer of W₂Se₁₀^{2-5,7} ((Se₂)(Se)W(μ-Se)₂W(Se)(Se₄)²⁻) (vs W₂S₁₀²⁻⁸). Those with no known sulfide analogues include W₂Se₉^{2-5,7} symmetrical W₂Se₁₀²⁻ ((Se₃)(Se)W(μ-Se)₂W(Se)(Se₃)²⁻),^{5,7} and V₂Se₁₃²⁻⁹. Routes to the Mo and W selenides begin with the MoSe₄²⁻¹ or WSe₄²⁻³ species, and these in turn were originally prepared from reactions of MoO₃ or WO₃ in concen-

trated aqueous ammonia solution with excess H₂Se. As the use of excess H₂Se is both expensive and dangerous, we have developed an alternative synthesis of these MSe₄²⁻ (M = Mo, W) ions. This involves the use of bis(dimethyloctylsilyl) selenide ((dmos)₂Se) as the source of selenium in place of H₂Se. We describe this alternative synthesis here.

The ions MQ(S₄)₂ⁿ⁻ [Q = O, S; M = Mo (n = 2),¹⁰ Re (n = 1)¹¹] are known. Here we describe the synthesis and characterization of the ions MoQ(Se₄)₂²⁻ and WQ(Se₄)₂²⁻ (Q = O, S, Se), starting from the MSe₄²⁻ ions. While these Mo selenides are directly analogous to their sulfur counterparts, the W selenides have no known corresponding sulfide analogues.

Experimental Section

All solvents and reagents were used as obtained. Reactions were routinely carried out with the use of standard Schlenk-line procedures under an atmosphere of dry dinitrogen. Microanalyses were performed by Galbraith Laboratories, Inc., Knoxville, TN, or by Analytical Laboratories, Engelskirchen, FRG. Na₂MoO₄·2H₂O, [NH₄]₂[WO₄], and (CH₃)₂(CH₃(CH₂)₇)SiCl were purchased from Aldrich Chemical Co., Milwaukee, WI. Li₂Se was prepared by the method of Gladysz et al.,¹² and Se₄(NC₅H₁₀)₂ and red selenium (Se₈) were prepared by the method of Foss and Janickis.¹³

- Müller, A.; Krebs, B.; Diemann, E. *Angew. Chem., Int. Ed. Engl.* **1967**, *6*, 257-258.
- Müller, A.; Diemann, E.; Jostes, R.; Bögge, H., *Angew. Chem., Int. Ed. Engl.* **1981**, *20*, 934-955.
- Lenher, V.; Fruehan, A. G. *J. Am. Chem. Soc.* **1927**, *49*, 3076-3080.
- Strasdeit, H.; Krebs, B.; Henkel, G. *Inorg. Chim. Acta* **1984**, *89*, L11-L13.
- Wardle, R. W. M.; Bhaduri, S.; Chau, C.-N.; Ibers, J. A. *Inorg. Chem.* **1988**, *27*, 1747-1755.
- Müller, A.; Rittner, W.; Neumann, A.; Königer-Ahlborn, E.; Bhattacharyya, R. G. *Z. Anorg. Allg. Chem.* **1980**, *461*, 91-95.
- Wardle, R. W. M.; Chau, C.-N.; Ibers, J. A. *J. Am. Chem. Soc.* **1987**, *109*, 1859-1860.
- Müller, A.; Römer, M.; Römer, C.; Reinsch-Vogell, U.; Bögge, H.; Schimanski, U. *Monatsh. Chem.* **1985**, *116*, 711-717.
- Chau, C.-N.; Wardle, R. W. M.; Ibers, J. A. *Inorg. Chem.* **1987**, *26*, 2740-2741.

- Draganjac, M.; Simhon, E.; Chan, L. T.; Kanatzidis, M.; Baenziger, N. C.; Coucouvanis, D. *Inorg. Chem.* **1982**, *21*, 3321-3332.
- Müller, A.; Ulrichmeyer, E.; Bögge, H.; Penk, M.; Rehder, D. *Chimia* **1986**, *40*, 50-52.
- Gladysz, J. A.; Hornby, J. L.; Garbe, J. E. *J. Org. Chem.* **1978**, *43*, 1204-1208.